Photosystem regulation in coral-associated dinoflagellates (Symbiodiniaceae) is the primary mode for seasonal acclimation

Colin J. Anthony[1], Colin Lock[1], Brett M. Taylor[1], Bastian Bentlage[1,*]

[1]*Marine Laboratory, University of Guam, Mangilao, Guam, USA*

* Correspondence: bentlageb@triton.uog.edu

Abstract

The collapse of the coral-dinoflagellate relationship under stress, as, for example, induced by increasing sea surface temperatures due to climate change, leads to coral bleaching and coral mortality. While symbiont shuffling or community shifting has been put forth as a rapid adaptive mechanism in corals, reported instances of these phenomena typically focus on environmental extremes rather than natural seasonal increases in sea surface temperatures that may lead to thermal stress, requiring regulation and acclimation of endosymbiotic Symbiodiniaceae. Understanding the dynamic nature of Symbiodiniaceae endosymbiont community responses to seasonal environmental fluctuations is necessary to help predict the limits of acclimation and adaptation potential. We used a combination of flow cytometry, 3D scanning, and ITS2 DNA metabarcoding to quantify *Acropora pulchra* Symbiodiniaceae community assemblage composition and function *in situ* in Guam (Micronesia). Samples were collected during the onset of seasonal warming and the time of year during which corals experience the highest sea water temperatures. Flow cytometry allowed us to expediently generate physiological profiles for thousands of individual endosymbiont cells using their autofluorescent signatures. Under variable environmental conditions, Symbiodiniaceae assemblages displayed site and season-specific photophysiological acclimation signatures while community composition and cell densities in host tissues remained homogeneous across sites. Variable photoacclimation patterns during the early season was followed by an island-wide convergence of photophysiological acclimation signatures during the season that sees the highest water temperatures in Guam. Our results show that photoacclimation rather than symbiont community assemblage reorganization allows for acclimation of *Acropora pulchra* to seasonal extremes in water temperatures.

Keywords: flow cytometry, coral reefs, fluorescence, symbiosis, photosynthesis, acclimation

Introduction

The ecological success of reef-building corals (Scleractinia) can be attributed to the endosymbiotic relationship between corals and their dinoflagellate endosymbionts (Symbiodiniaceae), a relationship that has evolved independently multiple times (Gault et al. 2021). Corals depend on these micro-algal endosymbionts for nutrient acquisition and effective calcification (Roth 2014), but environmental stress can lead to a functional breakdown of this photo-endosymbiotic relationship, leading to the expulsion of Symbiodiniaceae from the host (coral bleaching) (Brown 1997). Climate change has increased the frequency and severity of coral bleaching globally (Hughes et al. 2017). The survival of corals in stressful environments can be linked to differences in the ecological tolerances of Symbiodiniaceae (Parkinson and Coffroth 2015; Thornhill et al. 2014). If the environment shifts, and endosymbionts are not functionally advantageous, successful acclimation is commonly attributed to shifts in endosymbiont community composition, known as symbiont shuffling (Jones et al. 2008; Baker 2003; Buddemeier and Fautin 1993). However, Symbiodiniaceae community composition can be remarkably stable (Rouzé et al. 2019) suggesting alternative modes of acclimation, such as the upregulation of oxidative stress-reducing proteins (Maor-Landaw and Levy 2016).

Despite a large body of research on Symbiodiniaceae function and diversity, little is known about Symbiodiniaceae photophysiological acclimation *in situ*. Dinoflagellates can reorganize their photopigments and adjust morphology to acclimate to different light conditions (Johnsen et al. 1994; Xiang, 2015). However, prolonged light stress can lead to persistent damage of the Symbiodiniaceae photosystem (Berg et al. 2021). While coral bleaching has been proposed as a mechanism to survive unpredictable change (Baker 2001), Symbiodiniaceae experience no decline in photopigment abundance during coral bleaching (Venn et al. 2006;

Jeffrey & Humphrey. 1975). In recent decades, researchers have largely focused on understanding coral endosymbiont dynamics under extreme environmental stress, such as coral bleaching, thereby creating a potential knowledge gap in Symbiodiniaceae ecological tolerances and acclimation dynamics.

To elucidate the scales and mechanisms of Symbiodiniaceae acclimation in corals under natural conditions, we quantified the biodiversity, density, and photophysiology of Symbiodiniaceae in *Acropora pulchra* at the end of the cooler dry season and in the middle of the hotter wet season. *A. pulchra* is a dominant ecosystem engineer of Indo-Pacific and Pacific reef flat communities and has been described as having a 'flexible' Symbiodiniaceae assemblage (Rouzé et al. 2017). However, we found that Symbiodiniaceae community composition and cell densities in tissues were stable across space and time, while photophysiology varied with site and season suggesting within-cell photopigment regulation as the main mode of seasonal acclimation.

Materials and Methods

Field Sites. To identify the dynamics of Symbiodiniaceae assemblages under natural seasonal fluctuation, four thickets of *A. pulchra* from five reef flats (20 thickets total) were GPS-tagged and sampled around the island of Guam (Micronesia): Urunao (N 13.63672° E 144.84527°), West Agaña (N 13.47993° E 144.74278°), Luminao (N 13.46584° E 144.64496°), Togcha (N 13.36865° E 144.774967°), and Cocos Lagoon (N 13.24596° E 144.68475°) (Figure 1). *A. pulchra* was identified using a combination of population genetics (Rios 2020) and corallite morphology. Guam has distinct windward (East) and leeward sides (West). Urunao (North) is a pristine, shallow site with dense thickets of *A. pulchra* evenly distributed from the algal-

dominated reef crest to the beach. West Agaña (Northwest) has a large community of *A. pulchra* exposed to moderate wave energy. Luminao (West) has a small, scattered population of reasonably large thickets nested within an extensive *Porites*-dominated reef with a gentle, steady current driven by strong wave energy on a distant algal ridge. Cocos Lagoon (South) has a few small thickets of *A. pulchra* growing within the lagoon surrounded by sediment and massive *Porites* or within extensive, shallow water *Acropora aspera* thickets near the edge of the lagoon. The only known east-coast population of *A. pulchra*, Togcha (East), is limited to a few remaining thickets in the high wave energy zone near the reef crest.

Environmental Data. To characterize seasonal environmental changes, island-wide average sea surface temperature (SST) (NOAA Coral Reef Watch 2019) and precipitation (Menne et al. 2012a; Menne et al. 2012b) were obtained for 2021; bleaching risk was assessed using NOAA's virtual field station for Guam (Liu et al. 2018). Additionally, historical wave height, period, and cardinal direction were downloaded for 2012-2022 from wave buoys at Ritidian Point (N Guam) and Ipan (SE Guam), provided by the Pacific Islands Ocean Observing System (PacIOOS; www.pacioos.org).

Tissue Sampling. Coral tissue samples were collected at least three centimeters below the axial growth tip, flash-frozen in the field with liquid nitrogen, and stored at -80 °C until further processing. Three technical replicates per colony were collected from 20 tagged colonies during two time periods: 30 April - 18 May (1) and 28 July - 15 August 2021 (2).

Symbiodiniaceae biodiversity. Genomic DNA was extracted using a Qiagen DNeasy PowerSoil Pro Kit (Qiagen, Hilden, Germany) on a Qiacube connect liquid handling system. The ITS2 region was amplified via PCR with SYM_VAR_5.8S2 and SYM_VAR_REV primers (Hume et

al. 2018) using 3 µL of DNA (10 ng/µl), 3 µl of 10 µM primer, 2.4 µl of 2.5 mM dNTP, 18.6 µl water, 3 µl buffer (10x), and 0.15 units Taq (TaKaRa Taq™ DNA Polymerase 1U). The PCR profile was 26 cycles of 95°C for 40 s, 59°C for 120 s, 72°C for 60 s, and a final extension at 72°C for 420 s. ITS2 amplicons were multiplexed and sequenced on a NovaSeq 6000 (250bp Paired-end; Illumina, San Diego, CA, USA). Paired-end reads were initially analysed using the SymPortal pipeline with default parameters (Hume et al. 2019) to identify Symbiodiniaceae lineages and assign ITS2 type profiles.

Symbiodiniaceae density. Coral tissue was airbrushed from the skeleton with filtered seawater (FSW) and homogenised using a vortexer and syringe needle-shearing. One ml of tissue homogenate was transferred to 1.5 ml tubes and the remaining volume of tissue homogenate was measured with a graduated cylinder. Modified from the cytometry method described in Krediet et al. (2015), tissue homogenates were vigorously shaken for five seconds using a MiniBeadBeater Plus to separate Symbiodiniaceae cells from host cells and mucus, then centrifuged at 5000 rpm for four minutes at 10 °C. The supernatant was discarded, and the pellet of Symbiodinaceae cells was resuspended in 1 ml of FSW. Shaking (5 s) and centrifugation (3 min) was repeated. The supernatant was discarded and the pellet was resuspended in 1 ml of sodium dodecyl sulphate (SDS) solution (0.08% w/v SDS, 7/8 deionized water (DI), 1/8 FSW). Samples were diluted 1:10 with a 50:50 DI:FSW solution (Total volume: 200 µl) for flow cytometry. Symbiodinaceae concentrations (cells/ml) were estimated using two technical replicates with a Luminex Guava easyCyte 6HT-2L flow cytometer (Luminex Corporation, Austin, TX). Symbiodiniaceae were identified using red fluorescent emission (695±50 nm) from blue light excitation (488 nm laser) and side scatter (Krediet et al. 2015). Absolute cell counts were obtained by multiplying cytometry-generated cell concentrations by each sample's dilution

factor and tissue homogenate volume to determine total cell count for each coral tissue fragment. Cell densities per cm^2 (Equation 1) were obtained by the normalization of cell counts to the skeletal surface area. To generate a 3D model for each coral fragment, point clouds with 0.010 mm point spacing were generated using a 3D scanner (D3D-s, Vyshneve, Ukraine). Coral fragments were coated with SKD-S2 Aerosol (Magnaflux, Glenview, IL) to reduce skeletal light refraction. Point clouds of each fragment were imported into MeshLab v2020.04 (Cignoni et al. 2008) to generate a surface mesh by Poisson surface reconstruction. Portions of the fragment that were not covered in tissue prior to airbrushing were removed from the reconstructed surface prior to surface area estimation.

$$(1)\ \textit{Cell Density} = \frac{\textit{Cell Count} \cdot \textit{Dilution} \cdot \textit{Total Homogenate Volume}}{\textit{Sample Surface Area}}$$

Symbiodiniaceae fluorescent signatures. To characterize the physiological profile of individual dinoflagellate cells, we developed a protocol that quantifies Symbiodiniaceae photosystem components while counting cells using flow cytometry (Anthony et al., 2022). After identifying Symbiodinaceae cells, relative fluorescent intensity (RFI) of each cell was measured and averaged for the community. Two excitation/emission profiles were used to quantify red fluorescence. RED-B measured red emission (695/50 nm) off the blue (488 nm) excitation laser, while RED-R measured red RFI (661/15 nm) off the red (642 nm) excitation laser. Symbiodiniaceae possess two major light harvesting complex (LHC) antennae, the peridinin-chlorophyll a protein complex (PCP) and the chlorophyll a-chlorophyll c2-peridinin protein complex (acpPC), which use peridinin and chlorophyll c2 (chl c2) as the primary light-harvesting pigments (Polívkaa et al. 2007; Hiller et al. 1993). Red light emission caused by excitation with a blue laser (RED-B) represents peridinin in the PCP or acpPC LHC antenna complex (Jiang et al.

2012; Bujak et al. 2009). Red light emission caused by excitation with the red laser (RED-R) represents the other antennae components, as a hybrid emission/excitation signature of chlorophyll *a* and chlorophyll c_2 (chl *a* & chl c_2) (Niedzwiedzki et al. 2014; Yacobi 2012; Zapata et al. 2001). The combination of both red fluorescent (RED-B and RED-R) signatures are referred to as 'LHC pigments' herein.

Green fluorescence (525/30 nm) was measured off the blue (488 nm) excitation laser (GRN-B) and was identified as a hybrid signature of beta-carotene (Lee et al., 2019; Alwis et al., 2015; Lee et al., 2012; Kleinegris et al., 2010), xanthophylls (diadinoxanthin and diatoxanthin) (Kagatani et al. 2022; Frank et al. 1996), and flavin-based fluorescent proteins (FbFPs) (Mukherjee et al. 2013; Koziol et al. 2007; Fujita et al. 2005). Given the role of beta-carotene as an efficient antioxidant (Burton, 1990), the xanthophyll cycle's concurrence with antioxidant production (Smerilli et al. 2016), and FbFPs association with antioxidant accumulation (Deng et al. 2013; Taheri and Tarighi 2010; Sandoval et al. 2008), we refer to the green fluorescent signature (GRN-B) as 'antioxidant pigments'.

Statistical Analysis. Symbiodiniaceae community structure was compared across sites (North, Northwest, West, South, East) and seasons (May, August). Modelled after Eckert et al. (2020) using SymPortal relative ITS2 sequence abundances and type profiles that were normalized and visualized. Multivariate homogeneity of dispersion (PERMDISP), pairwise permutation tests, and a permutational multivariate analysis of variance (PERMANOVA) were conducted on normalized ITS2 type profiles using Vegan v2.5-7 (Oksanen et al. 2020) and pairwise Adonis v0.4 (Martinez Arbizu 2017) packages. PERMDISP used Bray-Curtis similarity and permutation tests used Bray-Curtis dissimilarity. Permutation tests were run with 9999 replicates.

Physiological data violated the assumption of parametric tests of a normal data distribution, as determined by Shapiro-Wilk tests. Therefore, to evaluate factorial contributions to Symbiodiniaceae physiology, repeated measures, multivariate analyses of variance and univariate analyses of variance (RM-MANOVA & RM-ANOVA) were performed to evaluate the response of cell density, chlorophylls, peridinin, and antioxidants using the MANOVA.RM package v0.5.3 (Friedrich et al. 2022). This test neither assumes multivariate normality nor covariance matrix specificity, making it robust to repeated measure designs with factorial nesting (Friedrich et al. 2019). A repeated measures MANOVA was performed on all factorial levels [Time*Site*Plot] with a multivariate combination of cell density, peridinin, chlorophylls, and antioxidant pigments. Univariate RM-ANOVAs were performed to evaluate factorial contributions for each physiological characteristic. Main and interaction effects were resampled with 1000 non-parametric bootstrap replicates and corrected p-values were generated for modified ANOVA-type statistics. To manually compare distribution means of interest across time and site, non-parametric Kruskal-Wallis tests (X^2) were performed using the FSA package v0.9.3 (Ogle et al. 2022). Given that chl *a*, chl c_2, and peridinin co-occur within major LHCs, linear regressions were generated to compare trends in chlorophyll and peridinin fluorescence. Principal component analysis (PCA) was used to visualize the overall data structure and further reveal sources of variation. The reduced-dimension data structure was visualized using ggbiplot v0.55 (Vu, 2011). All statistical analyses were completed with R v4.1.2 (R Core Team 2021) in RStudio v1.3.1073 (RStudio Team 2020). Figures were generated and modified with a combination of ggplot2 v3.3.5 (Wickham 2016), ggpubr v0.4.0 (Kassambara 2020), and InkScape v1.1 (https://inkscape.org).

Results

Environment. Wave energy on Guam was highest from December to March with waves, on average, coming from the East year-round (Figure 2a), the island's windward side. In 2021, Guam did not enter a coral bleaching warning (NOAA Coral Reef Watch 2019), and no bleaching was observed or reported. Therefore, 2021 represents a year characterized by natural seasonal fluctuations. Water temperature increased steadily from March to June, remaining stable during the following four months. Precipitation followed a similar trend (Figure 2b). May represented a seasonal transition with warming waters and decreasing wave energy; August was characterized by environmental stasis with high water temperatures and low wave energy (Figure 2b).

Symbiodiniaceae community. ITS2 metabarcoding yielded at least six replicates per site for each time point. However, plot replication was sometimes limited to a single sample, thus limiting interpretations to site level trends. Symbiodiniaceae communities of *A. pulchra* were largely dominated by *Cladocopium* C40 (Figure 3a). Beta-diversity dispersion was determined by site and not by time (Site: $F = 11.725$, $p < 0.001$; Time: $F = 0.0141$; $p = 0.9056$); biodiversity was stable with time ($F = 0.437$, $R2 = 0.00489$, $p = 0.7612$) (Figure 3a). Instead, Symbiodiniaceae communities were structured by site ($F = 88.793$, $R2 = 88.793$, $p = 0.001$) (Figure 3b). Pairwise permutation tests revealed North as an outlier, as it was the only site with a *Durusdinium* ITS2 type profile. A pairwise permutation test of the North across seasons indicated that communities were not statistically differentiated between sampling time points ($F = 0.5426815$, $R2 = 0.4945$, $p = 0.4945$). However, plot-specific data suggested *Cladocopium*/*Durusdinium* partitioning when comparing nearshore to farshore colonies, with *Durusdinium* being more common nearshore. ITS2 type profiles showed Symbiodiniaceae community overlap along Guam's western coast, while southern and eastern IT2 type profiles were distinct.

Symbiodiniaceae abundance and physiology. Using cell density, peridinin, chlorophylls, and antioxidants as multivariate components, season (RM-MANOVA: $t = 99.670$, $p < 0.001$) and site (RM-MANOVA: $t = 298.965$, $p = 0.001$) were the strongest contributors to variation (Table 1). Cell density only varied with time ($t = 291.668$, $p < 0.001$), though this was solely driven by a cell density shift at the southern site. LHC pigments were heavily influenced by time ($t = 291.668$, $p < 0.001$) and site ($t = 291.668$, $p < 0.001$); antioxidant pigments only by site ($t = 491.741$, $p < 0.001$) (Table 1). The North site showed signs of nearshore to farshore ITS2-type partitioning. Therefore, plots were compared to evaluate if ITS2-type profiles were associated with functional differences. Plots neither showed differences in cell density ($\chi2 = 7.2067$, df = 3, $p = 0.06559$) nor photophysiology (Flav: $\chi2 = 4.7533$, df = 3, p-value = 0.1908; Chl: $\chi2 = 1.2067$, df = 3, Car: p-value = 0.7514; $\chi2 = 1.7933$, df = 3, p-value = 0.6164). As such, ITS2 type-profiles were not likely to be relevant contributors to physiological data variation.

East coral colonies had much lower antioxidant and LHC pigments in May, but then converged with island-wide patterns by August (Figure 4b-e). Linear models of chlorophyll and peridinin autofluorescence confirmed a strong temporal, seasonal relationship (Figure 4e). One linear model best fit May corals ($R^2 = 0.765$; $p < 0.001$), while the other linear model predicted August corals ($R^2 = 0.555$; $p < 0.001$). An all encompassing linear model was still statistically supported ($R^2 = 0.457$; $p < 0.001$) of the variation. However, both timepoint-specific models had a better fit (R^2) to the data. Congruent with these linear models, pigments separated samples along the same PCA axis (PC1) that explained 55.9% of the variation in the data (Figure 4f). Separation of sites within time was apparent along PC1 (e.g. May:East, August:East, May: South, etc.) suggesting that photophysiology is influenced by both site and season. Cell density was the major factor of PC2, explaining 24.6% of the data variation (Figure 4f). However, no

factorial levels (Site, Time, nor Plot) structured along this axis, suggesting that variation in cell density is a result of natural colony-level variation rather than environmental differences between sites or seasons.

Discussion

We found that *Acropora pulchra* maintains a stable Symbiodiniaceae community across seasons from May, a transitional period with increasing water temperatures and decreasing wave energy, to August, a period of environmental stability with consistently high water temperatures and low wave action. Coral-dinoflagellate community acclimation is often associated with symbiont shuffling (changes in cell density or community composition) (Jones et al. 2008; Baker 2003), but we found limited evidence for seasonal symbiont shuffling. Instead, Symbiodiniaceae showed variable physiological profiles in May, a likely signal of environmental heterogeneity across sites during this period of seasonal change. Interestingly, physiological profiles converged across sites in August during environmental stasis with consistently elevated temperatures and reduced wave action (Figure 4). Given our observations, we presume that the the primary mode of seasonal acclimation in *A. pulchra* is Symbiodiniaceae photosystem regulation.

High community stability. We found that *A. pulchra*-associated Symbiodiniaceae communities were geographically structured and temporally stable (Figure 3). Long-term monitoring of endosymbiotic communities has described high stability and colony-level specificity (Rouze et al. 2019). However, this high fidelity in *A. pulchra* is surprising. In *Acropora*, Symbiodiniaceae are acquired from the environment (Baird et al. 2009), suggesting a more flexible and diverse assemblage compared to other coral genera (e.g. Qin et al. 2019; Rouzé et al. 2017). In contrast, coral colonies sampled by us were almost exclusively dominated by *Cladocopium* C40, with

only one site containing *Durusdinium* D1 (Figure 3). C40 and D1 represent important lineages associated with reduced coral bleaching rates and increased coral survival following stress (Qin et al. 2019; Rouzé et al. 2017; Mieog et al. 2009; Jones et al. 2008). The co-occurrence of D1-dominated and C40-dominated ITS2 type profiles within the North site (a narrow, shallow reef flat) suggests functional similarity. However, high thermotolerance in *Durusdinium* is associated with trade-offs, including decreased carbon and nitrogen fixation (Silverstein et al. 2017; Keshavmurthy et al. 2014; Stat et al. 2008), and increased volatile organic compound production (Lawson et al. 2019).

The dominance of *Cladocopium* C40 and *Durusdinium* D1 in *A. pulchra* on Guam's dynamic reef flats may be the result of selection, perhaps a result of recent environmentally driven mass coral mortality events (Raymundo et al. 2019; Raymundo et al. 2017). The original acquisition of C40 and D1 lineages could have occurred during coral larval settlement, increasing the likelihood of their survival during stress events (Suzuki et al. 2013), or the present *A. pulchra* community is composed of genets that successfully switched symbiont communities in response to extreme environmental stress (Buddemeier and Fautin 1993). Either way, *Acropora*-associated Symbiodiniaceae communities are determined by environmental filtering, and it is unlikely that symbiont shuffling is a mechanism for seasonal acclimation.

Photosystem dynamics. Peridinin RFI decreases from May to August in all colonies (Figure 4b) indicating an overall reduction of photopigments, a likely mechanism for acclimation to changing SSTs and photo-protection. Conversely, the incorporation of chlorophyll and antioxidant pigment signatures revealed divergent photophysiological profiles in May (Figure 4), suggesting variable acclimation responses to changing environmental conditions. The near-convergence of antioxidant and LHC profiles across sites in August (Figure 4) is likely a sign of

acclimation after environmental stabilization during the wet season that led to uniformly calm and warm waters around Guam. Similar dynamics have been described in many plants and algae (e.g. Bag et al. 2020; Orefice et al. 2016; Kolari et al. 2014; Porcar-Castell et al. 2008; Dietzel et al. 2008; Johnsen et al. 1994), which indicates that Symbiodiniacae use a common mechanism of seasonal photosystem regulation *in hospite*.

In May, windward colonies (East) displayed a reciprocal physiological profile compared to other sites. Despite this, photophysiology converged on leeward colonies by August (Figure 4). Interestingly, windward, East coral colonies displayed a distinctive green hue in May, presumably caused by green fluorescent protein (GFP) which was absent in August and not observed at other sites (Figure 4). Coral-host GFP expression has been linked to stress mitigation through shading of photosymbionts (Lyndby et al. 2016) and antioxidant activity (Palmer et al. 2009). *A. pulchra* occurs in a limited area near the East site's algal ridge, and is the only major population on the windward side of Guam. From December to May, the windward side experienced a high frequency of large swells (Figure 2a), which likely improved gas exchange (Finelli et al. 2006) and increased the availability of inorganic carbon, conditions that would increase the photosynthetic rates of coral endosymbionts (Dennison & Barnes 1988). However, if the coral host does not regulate its Symbiodiniaceae endosymbionts, the relationship can switch from symbiotic to parasitic (Morris et al. 2019). The visible expression of GFP coincided with low per cell antioxidant and LHC pigment RFIs (Figure 4b-d), suggesting that the coral host was regulating Symbiodiniaceae photophysiology (presumably with GFP) to avoid a breakdown of symbiosis. In late June, wave action decreased while SSTs increased (Figure 2). Following warming waters, decreased water flow, and increased rainfall, such host-mediated symbiont

photosystem regulation would be unnecessary, explaining convergence of East colonies with island-wide patterns of Symbiodiniaceae photophysiology.

Conclusions

We found limited evidence of seasonal symbiont shuffling (Figure 3, 4a). Instead, photosystem plasticity facilitated the acclimation of Symbiodiniaceae communities to seasonal environmental change across multiple reef sites (Figure 4b-f). In light of the physiological dynamics observed here, we posit that symbiont shuffling is an acclimation strategy to extreme or unpredictable change (acute stress), while photophysiological acclimation of existing Symbiodiniaceae is used under milder or predictable environmental change (chronic stress) such as changing seasonal conditions. Investigating photoacclimation dynamics of Symbiodiniaceae *in situ* in conjunction with host regulatory processes (e.g. ROS scavenging) will be an important next step to elucidate the dynamic and integrated nature of photoprotective mechanisms of the coral host and Symbiodiniaceae community. Additionally, we provide a foundation for identifying the ecophysiological response norms of Symbiodiniaceae acclimation to a changing environment, prior to the eventual breakdown of coral-dinoflagellate symbiosis under severe stress such as conditions of coral bleaching.

Acknowledgments

We wish to thank Dr. Cheryl Ames, Dr. Héloïse Rouzé, and Dr. Shinichiro Maruyama for providing their expertise and mentorship. We would also like to thank Marine Laboratory boat captain, Jonathan “Nanny” Perez, for assisting with field collections in Cocos Lagoon, and the Ritidian Eco Beach Resort for allowing land access to the pristine reef flats of Urunao. Wave data was provided by the Pacific Islands Ocean Observing System (PacIOOS)

(www.pacioos.org), which is a part of the U.S. Integrated Ocean Observing System (IOOS), funded in part by National Oceanic and Atmospheric Administration (NOAA) Awards #NA16NOS0120024 and #NA21NOS0120091. Guam NSF EPSCoR directly supported this work through National Science Foundation award OIA-1946352.

Author Contributions

CJA and BB conceived the ideas; CJA, BMT, and BB designed the experiment; CJA, CL, and BB collected field samples; CJA and CL developed lab protocols and generated data; CJA, CL, and BMT analysed the data; CJA led the writing of the manuscript. All authors contributed critically to the drafts and gave final approval for publication.

References

Anthony CJ, Lock CC, Bentlage B (2022) High-throughput physiological profiling of endosymbiotic dinoflagellates (Symbiodiniaceae) using flow cytometry. BioRxiv. https://doi.org/10.1101/2022.12.06.519248

Bag P, Chukhutsina V, Zhang Z, Paul S, Ivanov AG, Shutova T, Croce R, Holzwarth AR, Jansson S (2020) Direct energy transfer from photosystem II to photosystem I confers winter sustainability in Scots Pine. Nat Commun 11:6388. https://doi.org/10.1038/s41467-020-20137-9

Baird AH, Guest JR, Willis BL (2009) Systematic and biogeographical patterns in the reproductive biology of scleractinian corals. Annu Rev Ecol Evol Syst 40:551-571. https://doi.org/10.1146/annurev.ecolsys.110308.120220

Baker AC (2003) Flexibility and specificity in coral-algal symbiosis: Diversity, ecology, and biogeography of *Symbiodinium*. Annu Rev Ecol Evol Syst 34:661–689. https://doi.org/10.1146/annurev.ecolsys.34.011802.132417

Baker DM, Andras JP, Jordán-Garza, AG, Fogel ML (2013) Nitrate competition in a coral symbiosis varies with temperature among *Symbiodinium* clades. ISME J 7:1248–1251. https://doi.org/10.1038/ismej.2013.12

Berg JT, David CM, Gabriel MM, Bentlage B (2021) Fluorescence signatures of persistent photosystem damage in the staghorn coral *Acropora* cf. *pulchra* (Anthozoa: Scleractinia) during bleaching and recovery, Mar Biol Res 16(8-9):643-655. https://doi.org/10.1080/17451000.2021.1875245

Brown B (1997) Coral bleaching: causes and consequences. Coral Reefs 16:S129–S138. https://doi.org/10.1007/s003380050249

Buddemeier RW, Fautin DG (1993) Coral bleaching as an adaptive mechanism: A testable hypothesis. BioScience 43(5):320-326. https://doi.org/10.2307/1312064

Bujak Ł, Piatkowski D, Mackowski S, Wörmkeb S, Jungb C, Bräuchleb C, Agarwalc A, Kotovc NA, Schulted T, Hofmannd E, Brotosudarmoe THP, Scheere H, Govorovf AO, Hilleret RG (2009) Plasmon Enhancement of Fluorescence in Single Light-Harvesting Complexes from *Amphidinium carterae.* Acta Phys Pol 116:S22-S25. https://doi.org/10.12693/APhysPolA.116.S-22

Cignoni P, Callieri M, Corsini M, Dellepiane M, Ganovelli F, Ranzuglia G (2008) MeshLab: an Open-Source Mesh Processing Tool. Sixth Eurographics Italian Chapter Conference 129-136. https://doi.org/10.2312/LocalChapterEvents/ItalChap/ItalianChapConf2008/129-136

D'Amico-Damião V, Carvalho RF (2018) Cryptochrome-related abiotic stress responses in plants. Front Plant Sci 19. https://doi.org/10.3389/fpls.2018.01897

Deng B, Jin X, Yang Y, Lin Z, Zhang Y (2014) The regulatory role of riboflavin in the drought tolerance of tobacco plants depends on ROS production. Plant Growth Regul 72:269–277. https://doi.org/10.1007/s10725-013-9858-8

Dennison WC, Barnes DJ (1988) Effect of water motion on coral photosynthesis and calcification. J Exp Mar Biol Ecol 115:67–71. https://doi.org/10.1016/0022-0981(88)90190-6

Dietzel L, Bräutigam K, Pfannschmidt T (2008) Photosynthetic acclimation: State transitions and adjustment of photosystem stoichiometry – functional relationships between short-term and long-term light quality acclimation in plants. FEBS J 275:1080-1088. https://doi.org/10.1111/j.1742-4658.2008.06264.x

Entsch B, Ballou DP (2013) Flavins. Encyclopedia of Biological Chemistry, 309-313. https://doi.org/10.1016/B978-0-12-378630-2.00014-1

Finelli CM, Helmuth BST, Pentcheff ND, Wethey DS (2006) Water flow influences oxygen transport and photosynthetic efficiency in corals. Coral Reefs 25(1):47–57. https://doi.org/10.1007/s00338-005-0055-8

Frank, Cua A, Chynwat V, Young A, Gosztola D, Wasielewski MR (1996) The lifetimes and energies of the first excited singlet states of diadinoxanthin and diatoxanthin: the role of these molecules in excess energy dissipation in algae. Biochimica et Biophysica Acta. 1277:243-252.

Friedrich S, Konietshke F, Pauly M (2022) MANOVA.RM: Resampling-Based Analysis of Multivariate Data and Repeated Measures Designs. R package version 0.5.3. https://CRAN.R-project.org/package=MANOVA.RM

Friedrich S, Konietshke F, Pauly M (2019) Resampling-Based Analysis of Multivariate Data and Repeated Measures Designs with the R Package MANOVA.RM. R J 11(2):380-400. https://doi.org/10.32614/RJ-2019-051

Fujita S, Iseki M, Yoshikawa S, Makino Y, Watanabe M, Motomura T, Kawai H, Murakami A (2005) Identification and characterization of a fluorescent flagellar protein from the brown alga *Scytosiphon lomentaria* (Scytosiphonales, Pheophyceae): a flavoprotein homologous to Old Yellow enzyme. Eur J Phycol 40:159-167. https://doi.org/10.1080/09670260500063193

Gault JA, Bentlage B, Huang D, Kerr, AM (2021) Lineage-specific variation in the evolutionary stability of coral photosymbiosis. Sci Adv 7:eabh4243. https://doi.org/10.1126/sciadv.abh4243

Harrell Jr. FE (2021) Hmisc: Harrell Miscellaneous. R package version 4.6-0. https://CRAN.R-project.org/package=Hmisc

Hasler M, Kluss C (2019) SimComp: Simultaneous Comparisons for Multiple Endpoints. R package version 3.3. https://CRAN.R-project.org/package=SimComp

Hennige SJ, Suggett DJ, Warner ME, McDougall KE, Smith DJ. Photobiology of symbiodinium revisited: bio-physical and bio-optical signatures. Coral Reefs. 2009; 28:179-195. https://doi.org/10.1007/s00338-008-0444-x

Hiller RG, Wrench PM, Gooley AP, Shoebridge G, Breton J (1993) The major intrinsic light-harvesting protein of Amphidinium: Characterization and relation to other light-harvesting proteins. Photochem Photobiol, 57(1):125–131. https://doi.org/10.1111/j.1751-1097.1993.tb02267.x

Hughes TP, Barnes ML, Bellwood DR, Cinner JE, Cumming GS, Jackson JBC, Kleypas J, Kleypas J, van de Leemput, IA, Lough JM, Morrison TH, Palumbi SR, van Nes EH, Scheffer M (2017) Coral reefs in the Anthropocene. Nature 546:82–90. https://doi.org/10.1038/nature22901

Hume BCC, Ziegler M, Poulain J, Pochon X, Romac S, Boissin E, de Vargas C, Planes S, Wincker P, Voolstra CR (2018) An improved primer set and amplification protocol with increased specificity and sensitivity targeting the *Symbiodinium* ITS2 region. PeerJ 6:e4816. https://doi.org/10.7717/peerj.4816

Hume BCC, Smith EG, Ziegler M, Warrington HJM, Burt JA, LaJeunesse TC, Wiedenmann J, Voolstra C (2019) SymPortal: A novel analytical framework and platform for coral algal symbiont next-generation sequencing ITS2 profiling. Mol Ecol Resour 19(4):1063-1080. https://doi.org/10.1111/1755-0998.13004

Jiang J, Zhang H, Kang Y, Bina D, Lo CS, Blakeship RE (2012) Characterization of the peridinin–chlorophyll a-protein complex in the dinoflagellate *Symbiodinium*. Biochim Biophys Acta Bioenerg 1817(7):983-989. https://doi.org/10.1016/j.bbabio.2012.03.027

Jones AM, Berkelmans R, van Oppen MJH, Mieog JC, Sinclair W (2008) A community change in the algal endosymbionts of a scleractinian coral following a natural bleaching event: field evidence of acclimatisation. Proc Royal Soc B 275:1359–1365. https://doi.org/10.1098/rspb.2008.0069

Kagatani, K., Nagao, R., Shen, JR. et al. Excitation relaxation dynamics of carotenoids constituting the diadinoxanthin cycle. Photosynth Res (2022). https://doi.org/10.1007/s11120-022-00944-5

Kanazawa A, Blanchard GJ, Szabó M, Ralph PJ, Kramer DM (2014) The site of regulation of light capture in *Symbiodinium*: Does the peridinin–chlorophyll a–protein detach to regulate light capture? Biochim Biophys Acta Bioenerg, 1837(8):1227-1234. https://doi.org/10.1016/j.bbabio.2014.03.019.

Kassambara, A (2020) ggpubr: 'ggplot2' Based Publication Ready Plots. R package version 0.4.0. https://CRAN.R-project.org/package=ggpubr

Kolari P, Chan T, Porcar-Castell A, Bäck J, Nikinmaa E, Juurola E (2014) Field and controlled environment measurements show strong seasonal acclimation in photosynthesis and respiration potential in boreal Scots pine. Front Plant Sci 5. https://doi.org/10.3389/fpls.2014.00717

Kosumi D, Kusumoto T., Fujii R, Sugisaki M, Iinuma Y, Oka N, Takaesu,Y, Taira T, Iha M, Frank HA, Hashimoto H (2009) One- and two-photon pump–probe optical spectroscopic

measurements reveal the S1 and intramolecular charge transfer states are distinct in fucoxanthin. Chem Phys Lett 483(1-3):95–100. https://doi.org/10.1016/j.cplett.2009.10.077

Koziol B, Markowicz M, Kruk J, Plytycz B (2007) Riboflavin as a source of autofluorescence in *Eisenia fetida* coelomocytes. Photochem Photobiol 82(2):570-3. https://doi.org/10.1562/2005-11-23-RA-738

Krediet CJ, DeNofrio JC, Caruso C, Burriesci MS, Cella K, Pringle JR (2015) Rapid, Precise, and Accurate Counts of *Symbiodinium* Cells Using the Guava Flow Cytometer, and a Comparison to Other Methods. PLoS One 10(8):e0135725. https://doi.org/10.1371/journal.pone.0135725

Liu G, Eakin CM, Chen M, Kumar A, De La Cour JL, Heron SF, Geiger EF, Skirving WJ, Tirak KV, Strong AE (2018) Predicting heat stress to inform reef management: NOAA Coral Reef Watch's 4-Month Coral Bleaching Outlook. Front Mar Sci 5:57. https://doi.org/10.3389/fmars.2018.00057

Lyndby NH, Kühl M, Wangpraseurt D (2016) Heat generation and light scattering of green fluorescent protein-like pigments in coral tissue. Sci Rep 6:26599. https://doi.org/10.1038/srep26599

Maor-Landaw K, Levy O (2016) Survey of Cnidarian Gene Expression Profiles in Response to Environmental Stressors: Summarizing 20 Years of Research, What Are We Heading for?. In: Goffredo, S., Dubinsky, Z. (eds) The Cnidaria, Past, Present and Future. Springer, Cham. https://doi.org/10.1007/978-3-319-31305-4_32

Martinez Arbizu P (2017) pairwiseAdonis: Pairwise Multilevel Comparison using Adonis. R package version 0.4.

Maxwell K, Johnson GN (2000) Chlorophyll fluorescence - a practical guide. J Exp Bot 51(345):659-668. https://doi.org/10.1093/jexbot/51.345.659

Menne MJ, Durre I, Vose RS, Gleason BE, Houston TG (2012) An overview of the Global Historical Climatology Network-Daily Database. J Atmos Ocean Technol 29:897-910. https://doi.org/10.1175/JTECH-D-11-00103.1

Menne MJ, Durre I, Korzeniewski B, McNeal S, Thomas K, Yin X, Anthony S, Ray R, Vose RS, Gleason BE, Houston TG (2012) Global Historical Climatology Network - Daily (GHCN-Daily), Version 3.12. NOAA National Climatic Data Center http://doi.org/10.7289/V5D21VHZ [2022-04-15]

Mieog JC, Olsen JL, Berkelmans R, Bleuler-Martinez SA, Willis BL, van Oppen MJH (2009) The roles and interactions of symbiont, host and environment in defining coral fitness. PLoS One 4(7):e6364. https://doi.org/10.1371/journal.pone.0006364

Mukherjee A, Walker J, Weyant KB, Schroeder CM (2013) Characterization of Flavin-Based Fluorescent Proteins: An Emerging Class of Fluorescent Reporters. PLoS One 8(5):e64753. https://doi.org/10.1371/journal.pone.0064753

Niedzwiedzki DM, Jiang Jing CSL, Blankenship RE (2014) Spectroscopic properties of the Chlorophyll a–Chlorophyll c2–Peridinin-Protein-Complex (acpPC) from the coral symbiotic dinoflagellate *Symbiodinium*. Photosynth Res 120:125-139. https://doi.org/10.1007/s11120-013-9794-5

NOAA Coral Reef Watch (2019, updated daily) NOAA Coral Reef Watch Version 3.1 Daily 5km Satellite Regional Virtual Station Time Series Data for Guam, Jan. 1, 2021-Jan. 1, 2022. College Park, Maryland, USA: NOAA Coral Reef Watch. Data set accessed 2021-02-11 at https://coralreefwatch.noaa.gov/product/vs/data.php.

Ogle, D.H., J.C. Doll, P. Wheeler, and A. Dinno. 2022. FSA: Fisheries Stock Analysis. R package version 0.9.3, https://github.com/fishR-Core-Team/FSA.

Oksanen J, Blanchet FG, Friendly M, Kindt R, Legendre P, Minchin PR, Wagner H (2019) Vegan: Community Ecology Package. R package version 2.5–6. https://CRAN.Rproject.org/package=vegan

Oliveira CYB, Abreu JL, Santos EP Matos AP, Tribuzi G, Oliveira CDL,Veras BO, Bezerra RS, Müller MN, Gálvez AO (2022) Light induces peridinin and docosahexaenoic acid accumulation in the dinoflagellate *Durusdinium glynnii*. Appl Microbiol Biotechnol 106:6263–6276. https://doi.org/10.1007/s00253-022-12131-6

Oswald F, Schmitt F, Leutenegger A, Ivanchenko S, D'Angelo C, Salih A, Maslakova S, Bulina M, Schirmbeck R, Nienhaus GU, Matz MV, Wiedenmann J (2007) Contributions of host and symbiont pigments to the coloration of reef corals. FEBS J 274:1102–1109. https://doi.org/10.1111/j.1742-4658.2007.05661.x

Palmer CV, Modi CK, Mydlarz LD (2009) Coral fluorescent proteins as antioxidants. PLoS One, 4(10):e7298. https://doi.org/10.1371/journal.pone.0007298

Polivka T, Hiller RG, Frank HA (2007) Spectroscopy of the peridinin–chlorophyll-a protein: insight into light-harvesting strategy of marine algae. Arch Biochem Biophys 458: 111–120. https://doi.org/10.1016/j.abb.2006.10.006

Porcar-Castell A, Juurola E, Ensminger I, Berninger F, Hari P, Nikinmaa E (2008) Seasonal acclimation of photosystem II in *Pinus sylvestris*. II. Using the rate constants of sustained thermal energy dissipation and photochemistry to study the effect of the light environment. Tree Physiol 28(10):1483–1491. https://doi.org/10.1093/treephys/28.10.1483

Qin Z, Yu K, Chen B, Wang Y, Liang J, Luo W, Xu L, Huang X (2019) Diversity of Symbiodiniaceae in 15 coral species from the Southern South China Sea: Potential relationship with coral thermal adaptability. Front Microbiol 10:2343. https://doi.org/10.3389/fmicb.2019.02343

Raymundo LJ, Burdick D, Hoot WC, Miller RM, Brown V, Reynolds T, Gault J, Idechong J, Fifer J, Williams A (2019) Successive bleaching events cause mass coral mortality in Guam, Micronesia. Coral Reefs, 38:677–700. https://doi.org/10.1007/s00338-019-01836-2

Raymundo LJ, Burdick D, Lapacek VA, Miller R, Brown V (2017) Anomalous temperatures and extreme tides: Guam staghorn *Acropora* succumb to a double threat. Mar Ecol Prog Ser 564:47-55. https://doi.org/10.3354/meps12005

R Core Team. (2021). R: A language and environment for statistical computing. R Foundation for Statistical Computing, Vienna, Austria. https://www.R-project.org/

Rios D (2020) The population genetic structure of *Acropora pulchra* in Guam [Master's Thesis]. University of Guam. https://www.uog.edu/_resources/files/ml/theses/MLThesis_RiosD.pdf

Roth MS (2014) The engine of the reef: photobiology of the coral-algal symbiosis. Front Microbiol 5. https://doi.org/10.3389/fmicb.2014.00422

Rouzé H, Lecellier G, Pochon X, Torda G, Berteaux-Lecellier V (2019) Unique quantitative Symbiodiniaceae signature of coral colonies revealed through spatio-temporal survey in Moorea. Sci Rep 9:7921. https://doi.org/10.1038/s41598-019-44017-5

Rouzé H, Lecellier GJ, Saulnier D, Planes S, Gueguen Y, Wirshing HH, Berteaux-Lecellier V (2017) An updated assessment of *Symbiodinium* spp. that associate with common scleractinian corals from Moorea (French Polynesia) reveals high diversity among

background symbionts and a novel finding of clade B. PeerJ 5:e2856. https://doi.org/10.7717/peerj.2856

RStudio Team (2020) RStudio: Integrated Development for R. RStudio, PBC, Boston, MA. http://www.rstudio.com/

Sandoval FJ, Zhang Y, Roje S (2008) Flavin Nucleotide Metabolism in Plants. J Biol Chem 283(45):30890-30900. https://doi.org/10.1074/jbc.M803416200

Schulte T, Johanning S, Hofmann E (2010) Structure and function of native and refolded peridinin-chlorophyll-proteins from dinoflagellates. Eur J Cell Biol 89(12):990–997. https://doi.org/10.1016/j.ejcb.2010.08.004

Smerilli A, Orefice I, Corato F, Olea AG, Ruban AV, Brunet C (2016) Photoprotective and antioxidant responses to light spectrum and intensity variations in the coastal diatom *Skeletonema marinoi*. Environ Microbiol 19(2):611-627. https://doi.org/10.1111/1462-2920.13545

Stadnichuk IN, Tropin IV (2017) Phycobiliproteins: Structure, Functions and Biotechnological Applications. Appl Biochem Microbiol 53(1):1–10. https://doi.org/10.1134/S0003683817010185

Slavov C, Schrameyer V, Reus M, Ralph PJ, Hill R, Büchel C, Larkum AWD, Holzwarth AR (2016) "Super-quenching" state protects *Symbiodinium* from thermal stress - Implications for coral bleaching. Biochim Biophys Acta Bioenerg 1857:840–847. https://doi.org/10.1016/j.bbabio.2016.02.002

Stat M, Morris E, Gates RD. (2008). Functional diversity in coral–dinoflagellate symbiosis. Proc Natl Acad Sci USA 105(27): 9256–61. https://doi.org/10.1073/pnas.0801328105

Taheri P, Tarighi S (2010). Riboflavin induces resistance in rice against *Rhizoctonia solani* via jasmonate-mediated priming of phenylpropanoid pathway. J Plant Physiol 167:201–208. https://10.1016/j.jplph.2009.08.003

Tanaka K, Iida S, Takaichi S, Mimuro M, Murakami A, Akimoto S (2016) Excitation relaxation dynamics and energy transfer in pigment–protein complexes of a dinoflagellate, revealed by ultrafast fluorescence spectroscopy. Photosynth Res 130:183–191. https://doi.org/10.1007/s11120-016-0238-x

Venn AA, Wilson MA, Trapido-Rosenthal HG, Keely BJ, Douglas AE (2006) The impact of coral bleaching on the pigment profile of the symbiotic alga, *Symbiodinium*. Plant Cell Environ 29:2133-2142. https://doi.org/10.1111/j.1365-3040.2006.001587.x

Weston AJ, Dunlap WC, Shick JM, Klueter A, Iglic K, Vukelic A, Starcevic A, Ward M, Wells ML, Trick CG, Long PF (2012) A profile of an endosymbiont-enriched fraction of the coral *Stylophora pistillata* reveals proteins relevant to microbial-host interactions. Mol Cell Proteomics 11(6). https://doi.org/10.1074/mcp.M111.015487-2

Wickham H (2016) ggplot2: Elegant Graphics for Data Analysis. Springer New York. https://doi.org/10.1007/978-0-387-98141-3

Yacobi YZ (2012) From Tswett to identified flying objects: A concise history of chlorophyll a use for quantification of phytoplankton. Isr J Plant Sci 60(1). https://doi.org/10.1560/IJPS.60.1-2.243

Yu X, Liu H, Klejnot J, Lin C (2010) The Cryptochrome Blue Light Receptors. Arabidopsis Book 8:e0135. https://doi.org/10.1199/tab.0135

Zapata M, Edvardsen B, Rodriguez F, Maestro MA, Garrido JL (2001) Chlorophyll c_2 monogalactosyldiacylglyceride ester (chl c_2- MGDG). A novel marker pigment for

Chrysochromulina species (Haptophyta). Mar Ecol Prog Ser 219:85-98.

https://www.doi.org/10.3354/meps219085

Table headings and figure legends

Table 1: Results of repeated measures (RM) MANOVAs to estimate the factorial contributions site and time (season) to Symbiodiniaceae cell densities and relative fluorescence intensities of peridinin, chlorophylls, and antioxidants. Top: RM-MANOVA for combined effects on cell density, photo-pigments, and antioxdiants. Bottom: Effect of site and time on individual parameters (cell density, peridinin, chlorophylls, antioxidants).

	Cell, Per, Chl, Antiox	
	t	p
Time	99.67	<0.001*
Site	298.965	0.001*
Time:Site	260.957	0.006*
Site:Plot	79.185	0.306
Time:Site:Plot	57.477	0.421

	Cell Density	
	t	p
Time	49.56	0.018*
Site	0.619	0.515
Time:Site	1.249	0.366
Site:Plot	1.014	0.433
Time:Site:Plot	0.749	0.527
	Peridinin	
	t	p
Time	353.179	<0.001*
Site	67.181	0.002*
Time:Site	8.805	0.029*
Site:Plot	1.376	0.334
Time:Site:Plot	1.102	0.399
	Chlorophylls	
	t	p
Time	168.35	0.008*
Site	62.911	0.003*
Time:Site	23.915	0.015*
Site:Plot	1.745	0.272
Time:Site:Plot	0.67	0.537
	Antioxidants	
	t	p
Time	2.728	0.217
Site	14.111	0.022*
Time:Site	12.076	0.028*
Site:Plot	1.218	0.372
Time:Site:Plot	1.428	0.322

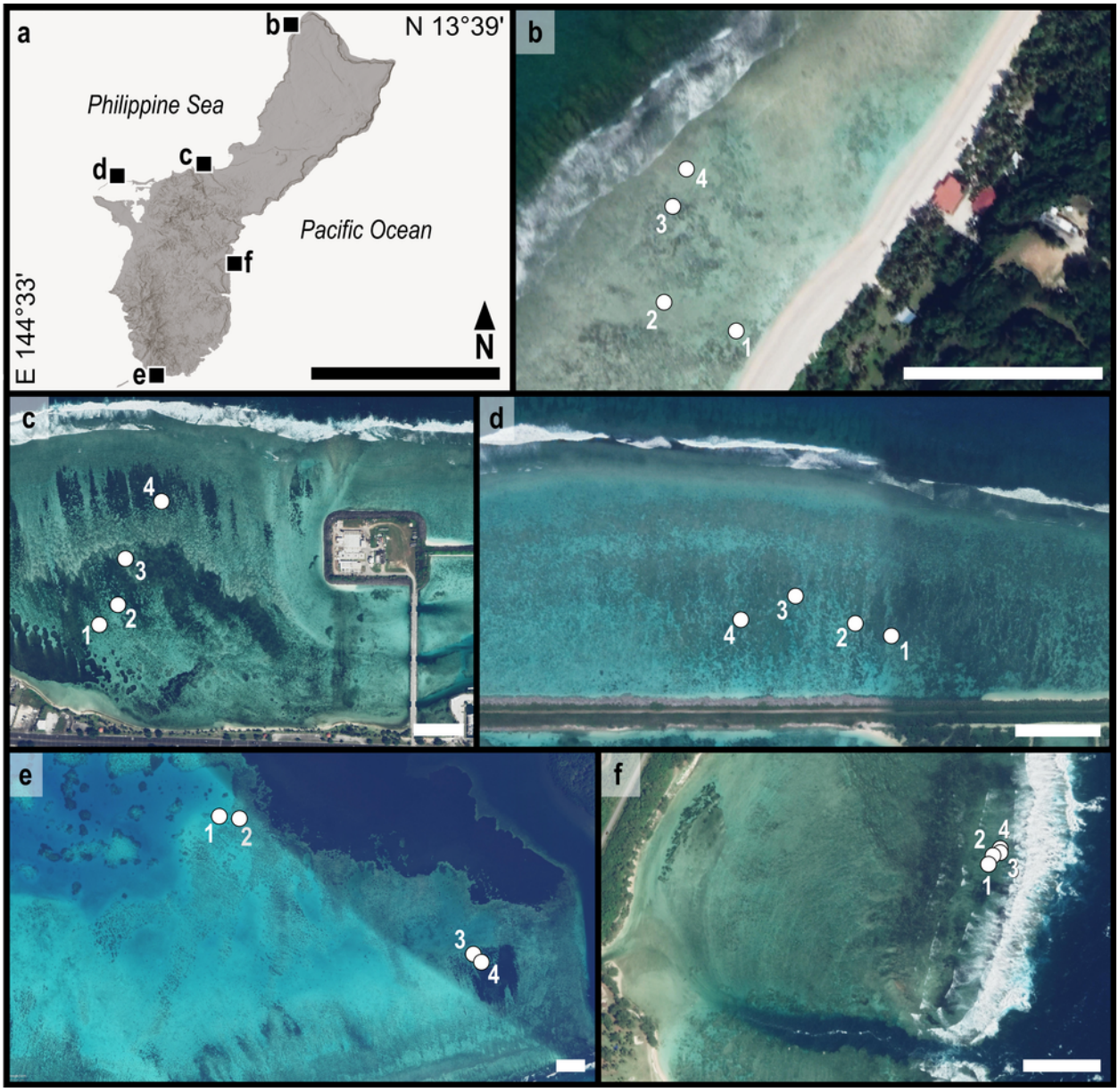

Figure 1: a) Sampling sites in Guam (scale: 20 km) with each square indicating the location of a reef flat sampled for this study: **b**) Urunao (N), **c**) West Agaña (NW), **d**) Luminao (W), **e**) Cocos Lagoon (S), and **f**) Togcha (E). **b-f**) Within each site, four thickets (**1-4**) of *A. pulchra* were georeferenced for repeated sampling. Images provided by Google Earth Pro v7.3.4.8248. (scale: 100 m)

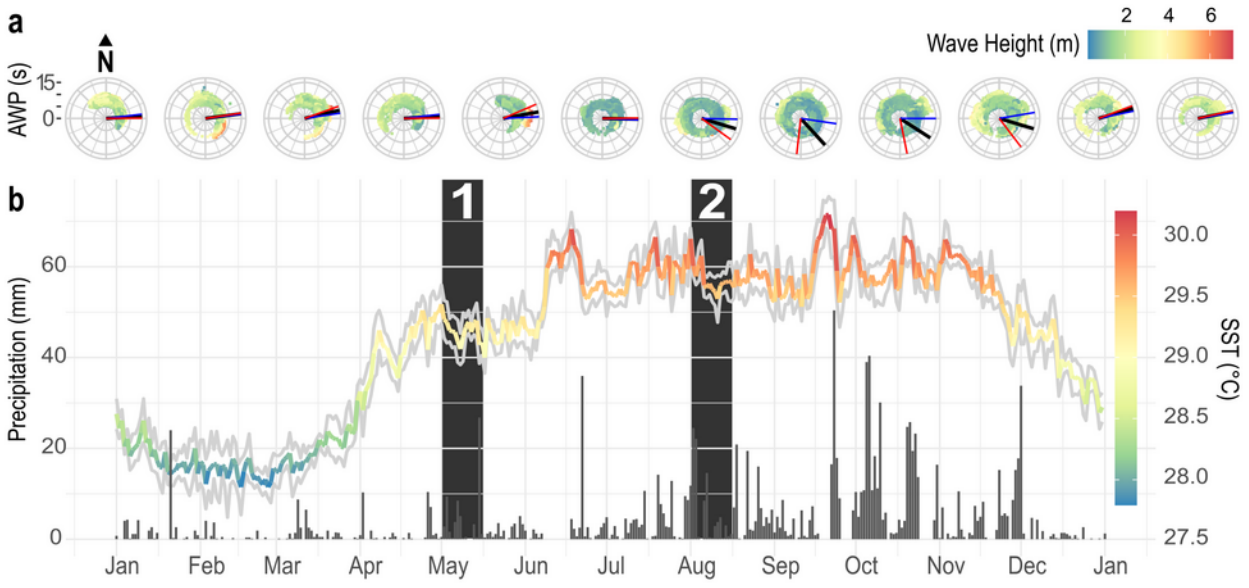

Figure 2: a) Spectral polar plots of aggregated historical wave data from Ritidian (**red lines**) and Ipan (**blue lines**) wave buoys. Monthly mean wave direction (**black lines**) indicated prevailing swells from the East, the windward side of Guam. Waves were higher with shorter periods from January to April, the season that sees strong westerly trade winds. (Provided by PacIOOS (www.pacioos.org)). **b**) Average sea surface temperature (SST) (**spectral line**) (NOAA Coral Reef Watch, 2019), and precipitation (**grey bars**) (Menne et al., 2012a; Menne et al., 2012b) for 2021 showed distinct seasonal patterns. The first set of samples was collected in the first two weeks of May (**1**) during the transitional warming period, while the second set of samples was collected in the first two weeks of August (**2**) during the hot, rainy season.

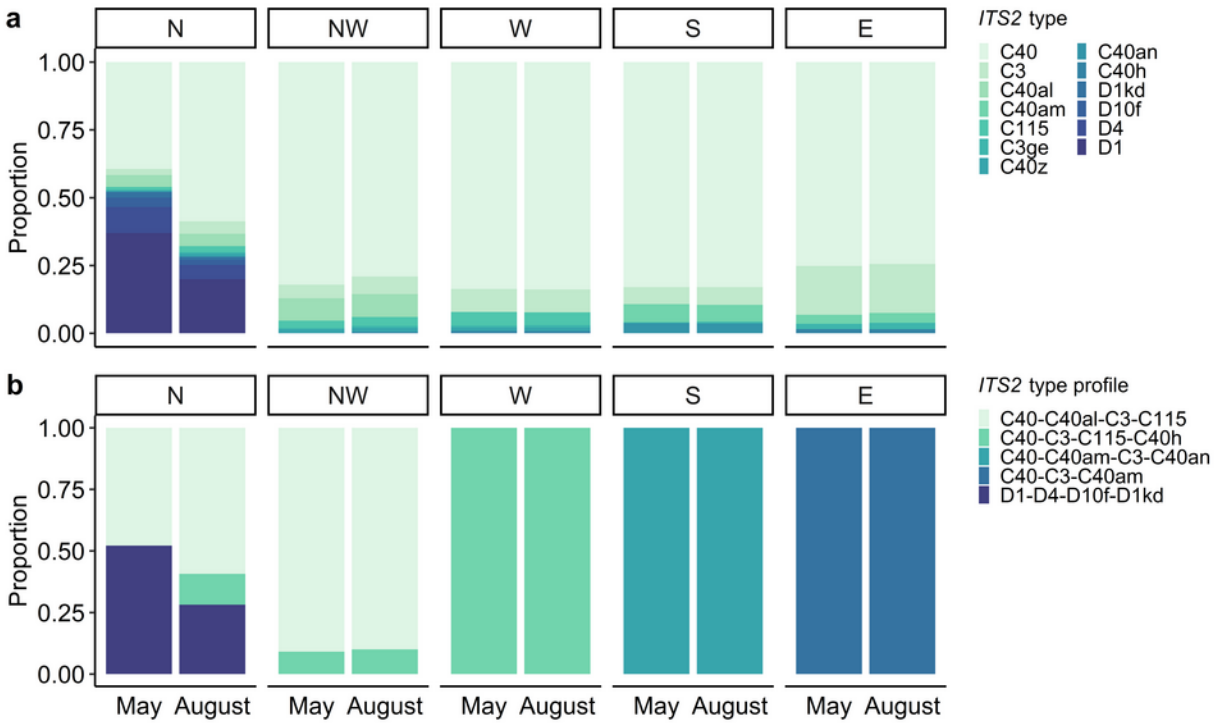

Figure 3: a) ITS2 type diversity for endosymbiotic Symbiodiniaceae revealed high community similarity across sites and seasons. *Cladocopium* C40 dominated all sites except for North. **b)** ITS2 type profiles differed between sites, with low abundance Symbiodiniaceae clades causing differences among profiles. ITS2 type profiles did not shift significantly over time, but were distinct between sites.

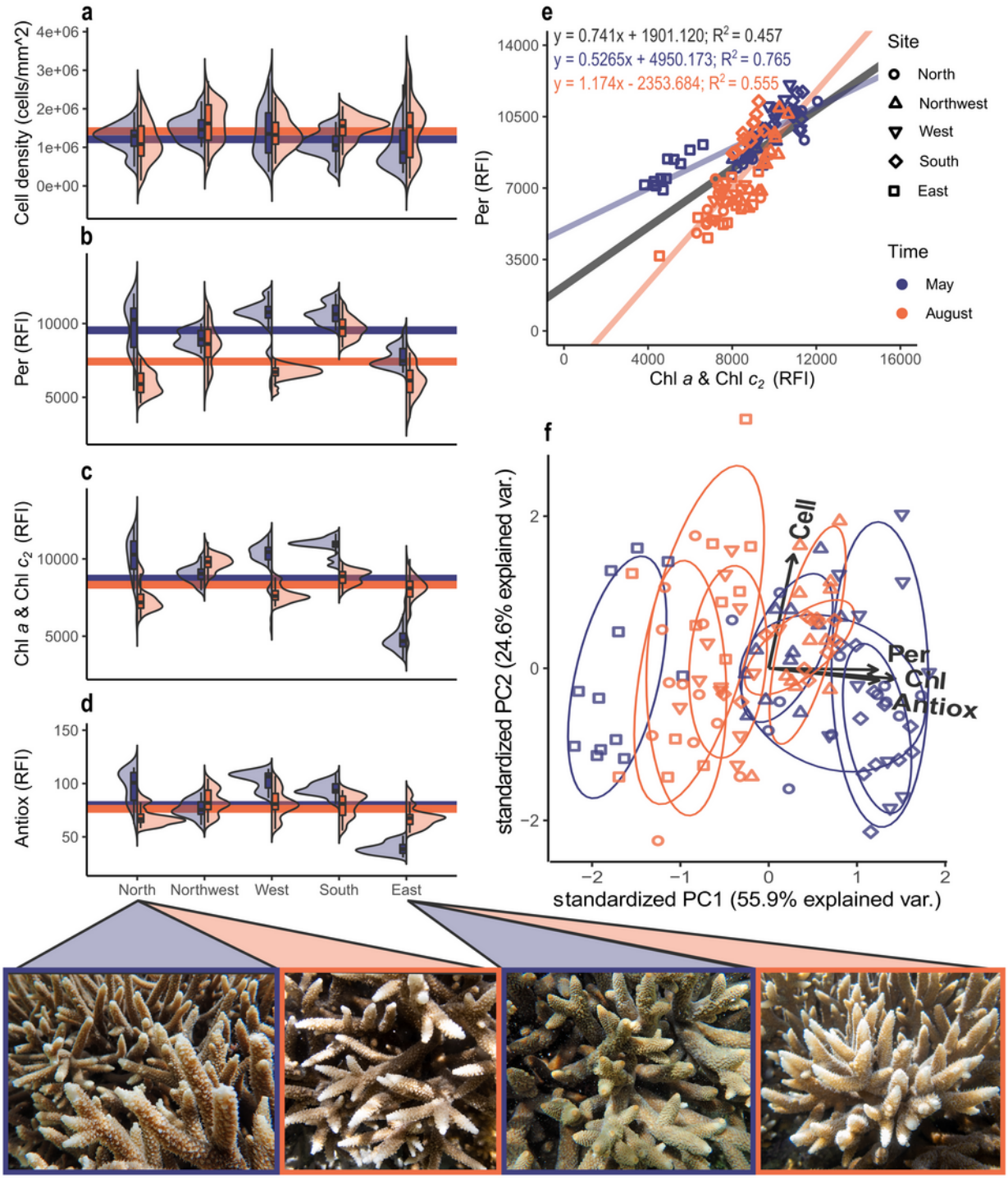

Figure 4: Cell density (**a)** was stable across sites during both May (**blue**) and August (**orange**). Peridinin (**b**), chl *a* & chl c_2 (**c**), and antioxidants (**d**) varied across sites and seasons. The East site displayed reciprocal autofluorescent signatures compared to the other sites. In May, East site

Acropora pulchra displayed a visible green hue likely caused by green fluorescent protein (GFP) expression in the coral host, which was not not observed at other sites or at other times. **e**) Peridinin and chlorophyll autoflueorescence covaried due to their association as part of the peridinin-chlorophyll a protein complex (PCP) and the chlorophyll a-chlorophyll c2-peridinin protein complex (acpPC) in the ligh harvesting complex (LHC) antennae. Shifts in slope across time may suggest a shift in LHC reorganization as a mechanism of seasonal acclimation. All three linear regressions were significant ($p < 0.001$). **f**) Principal Component Analaysis (PCA) showed that all photophysiological signatures measured explained the majority of the variation in the data variation (55.9%), separating samples along the first axis (PC1). Cell density explained 24.6% of data variation along the second axis (PC2). Sites nested within time (**ellipses**) were separated along PC1 while PC2 did not yield clusters that could be related to site or time, suggesting that photophysiology was the main mode of seasonal acclimation and variation in cell density observed represents natural variation between coral colonies.